Fifth International Conference on CFD in the Process Industries
CSIRO, Melbourne, Australia
13-15 December 2006

POPULATION BALANCE – CFD MODELLING OF FLUID FLOW, SOLIDS DISTRIBUTION AND FLOCCULATION IN THICKENER FEEDWELLS

Tuan NGUYEN, Alex HEATH, and Peter WITT

Parker Centre for Integrated Hydrometallurgy Solutions
(CSIRO Minerals) Clayton, Victoria 3169, AUSTRALIA

ABSTRACT

A population balance (PB)–CFD model has been used to describe fluid flow, solids distribution, and aggregation/breakage kinetics of flocculation in gravity thickeners. The behaviour and transport of flocculated solids from the feedwell to various points in the settling zone below the feedwell and also the settling rate are governed by the hydrodynamics, turbulent mixing, and flocculation within the feedwell. The PB model, developed from an extensive range of experimental data and validated in pilot-scale thickener feedwells, describes simultaneous aggregation and breakage as a function of various process variables, such as fluid shear, flocculant dosage, primary particle size and solid fraction. The model has been used to investigate the fluid flow structure, distributions of feed solids and aggregation in a full-scale thickener at different flow conditions. The investigation has provided significant new insights into the performance and operation of a gravity thickener.

NOMENCLATURE

a	Particle radius (m)
d	Particle diameter (m)
k	Turbulent kinetic energy ($m^2 s^{-2}$)
$\mathbf{U}$	Velocity ($m s^{-1}$)
t	Time (s)
N	Particle number density (m^{-3})
S	Source ($kg m^{-3} s^{-1}$)
S_i	Breakage kernel (s^{-1})

Greek

α	Capture efficiency (dimensionless)
β	Aggregation kernel ($m^{-3} s^{-1}$)
ε	Energy dissipation rate ($m^2 s^{-3}$)
ϕ	Volume fraction (dimensionless)
ρ	Density ($kg m^{-3}$)
Γ	Diffusivity ($kg m^{-1} s^{-1}$)
μ	Viscosity ($kg m^{-1} s^{-1}$)
ν	Kinematic viscosity ($m^2 s^{-1}$)

Subscripts

agg	Aggreate
p	Primary particle
i,j,k	Particle size group
α,β	Fluid phase

INTRODUCTION

Thickeners are a key unit in many hydrometallurgical processing operations and are used to separate solids and liquids. Flocculant is often added to cause bridging and particle agglomeration so that the larger agglomerates can settle producing a clear liquor overflow and a concentrated underflow suspension of solids. The overflow is usually collected from the outer edge of the upper surface of the thickener, and the thickened underflow is typically pumped through a centrally located drain at the base of the thickener.

The nature of the flow in the feedwells is of critical importance to the performance of industrial thickeners since it is generally here that most of the aggregation process occurs, due to the addition of flocculant. The flow here is turbulent, and the characteristics of the turbulence have a major influence on flocculant mixing and particle aggregation processes and consequently the size and density of aggregates that are formed.

A CFD feedwell model has been enhanced with the incorporation of Population Balance (PB) capability to account for aggregate growth and breakage processes (i.e. flocculation kinetics). The PB-CFD thickener model has been developed based on knowledge of the fundamental physical and chemical processes occurring within the thickener feedwell, that has been gained from a comprehensive range of experimental measurements conducted on the laboratory, pilot scale and full-scale. It has also been validated using LDV velocity measurements of flow fields in small scale feedwell models (see Sutalo *et al*., 2000 and 2001, White *et al*., 2003).

MODEL DESCRIPTION

A conventional steady-state Eulerian-Eulerian 2-phase model is used with the standard k-ε turbulence model acting in the continuous phase. The phases share a common pressure field, with the momentum equations coupled via the inter-phase drag due to the liquid-particle slip. Implementation is in CFX-4, with extensive use of additional Fortran to include the population balance and extra physics.

The population balance size distribution is modelled as a series (typically 35) of transported scalars associated with the second particle phase, i.e. all the scalars share the velocity field with the second phase although they are diffused according to their own concentration gradients and have their own population balance source terms:

$$\frac{\partial \phi_\beta \rho_\beta N_{\beta,i}}{\partial t} + \nabla \cdot \left[\phi_\beta \rho_\beta \mathbf{U}_\beta N_{\beta,i} - \Gamma_{x,\beta} \nabla \left(\phi_\beta N_{\beta,i} \right) \right] = \phi_\beta \rho_\beta S_\beta \quad (1)$$

Where S_β is the source term from the population balance, ie:

$$\frac{dN_i}{dt} = \sum_{j=1}^{i-2} 2^{j-i+1} \beta_{i-1,j} N_{i-1} N_j + \tfrac{1}{2} \beta_{i-1,i-1} N_{i-1}^2 - N_i \sum_{j=1}^{i-1} 2^{j-i} \beta_{i,j} N_j - N_i \sum_{j=i}^{\infty} \beta_{i,j} N_j - S_i N_i + \sum_{j=i}^{\infty} \Gamma_{i,j} S_j N_j \quad (2)$$

The aggregation kernel is the widely used turbulent collision kernel by Saffman and Turner (1956):

$$\beta_{ij} = 1.294 \alpha \sqrt{\frac{\varepsilon}{\nu}} \left(a_i + a_j \right)^3 \quad (3)$$

The capture efficiency (α) is determined from the local concentration of adsorbed flocculant, modelled as an additional transported scalar in both phases with inter-phase transfer given by the flocculant adsorption rate. The breakage kernel also includes the adsorbed flocculant level, expressed per unit particle surface area:

$$S_i = \frac{k_2 \varepsilon^{k_3} \mu d_i}{\theta_f} \qquad \overline{d_{agg}} > d_p$$
$$= 0 \qquad \overline{d_{agg}} \le d_p \quad (4)$$

Details of the population balance kernels, and their development from experimental data can be found in Heath *et al.* 2006A, and initial PB-CFD model implementation found in Heath and Koh 2003.

The resulting particle size distribution is then volume averaged and used to calculate the inter-phase drag via a modified Stokes (1851)/Richardson and Zaki (1955) hindered settling function, see Heath *et al.* 2006B. I.e. the inter-phase drag varies through the flow depending on the local aggregate size. The local volume weighted size is given by:

$$\overline{d_{agg}} = \frac{\sum_i N_i d_i^4}{\sum_i N_i d_i^3} \quad (5)$$

RESULTS

In this section, the nature of new insights that can be obtained from the use of the PB-CFD are demonstrated through simulations of a generic full-scale thickener fitted with an open feedwell with a single feed inlet entering the feedwell tangentially (**Figure 1**).

Thickener dimensions and operating conditions are:

- Thickener: 20 m diameter and 7 m height.
- Feedwell: 4 m diameter and 3 m height.
- Feedpipe: 500 mm diameter.
- Kinematic liquor viscosity of 10^{-6} m^2 s^{-1} and solids density of 2710 kg m^{-3}.
- Flocculant dosage of 20 g t^{-1}.
- PB system: calcite (Omyacarb 20), 30% anionic acrylamide/acrylate copolymer flocculant with high molecular weight.
- Feed flow rate which varies from 500 to 2000 m^3 h^{-1}.
- Feed solids concentration of 5% w/v (i.e. 50 g L^{-1} or kg m^{-3}).

The CFD images presented in the following sections include plan view plots, which show the distribution of selected variables at six slices covering the entire feedwell, from the free surface down to the exit plane. The vertical velocity is positive in the downward direction. In these figures, the feedwells were not plotted to scale, but were stretched in the vertical direction to adequately display all slices. The elevation view plots show the distribution of various variables at four slices covering the entire thickener at 90° intervals in the anti-clockwise direction.

From the PB-CFD model output, several parameters were calculated at a plane (see **Figure 1**), which has a diameter twice that of the feedwell and located in the settling zone (1 m below the exit of the feedwell). The reason to use this measurement plane rather than the feedwell exit plane is to take into account the effect of post-feedwell flocculation and to get a better estimate of what solids are reaching the bed below.

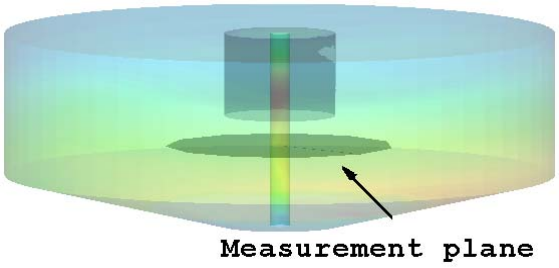

Figure 1: Schematic diagram of feedwell and thickener geometry and size and location of the measurement plane.

The PB-CFD model was used to study the effect of flow rate (500, 1000 & 2000 m^3 h^{-1}) on the flocculation performance for the open feedwell, with all other variables (solids loading of 5%w/v, flocculant dosage of 20 g t^{-1}, etc) held constant.

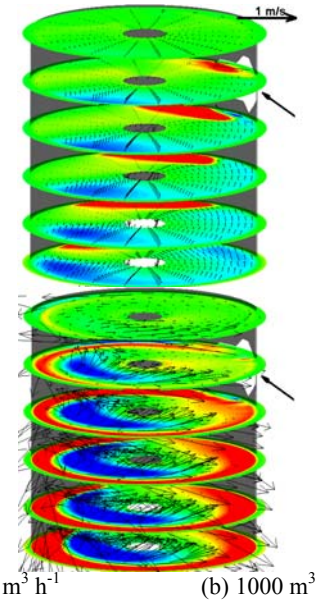

(a) 500 m^3 h^{-1} (b) 1000 m^3 h^{-1}

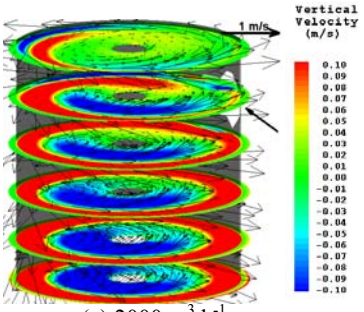

(c) 2000 m^3 h^{-1}

Figure 2: PB-CFD model prediction (plan views) of the vertical velocity depicting internal dilution in the open feedwell.

The feed flow rate greatly influences the flow behaviour and solids distribution within the feedwell as shown by the plots of the vertical velocity and solids concentration in **Figure 2** and **Figure 3**. The extent of internal dilution (i.e. the ingress of liquor from the bulk of the thickener into the feedwell - see blue contour levels) can be clearly seen in **Figure 2**. At the low flow rate (500 m^3 h^{-1}), the unrestrained feed stream tends to expand for only a short distance around the inner wall before gravity pulls it downward and out of the feedwell. This occurs as a result of the higher solids concentration of the feed stream, which makes it denser than the surrounding fluid. As the flow rate increases, the swirling feed stream can be clearly seen expanding more evenly around the feedwell walls, which promotes more mixing and higher solids concentrations inside the feedwell (**Figure 3**). This in turns creates an increasingly stronger dilution stream as indicated by the blue sections and upward-pointing velocity vectors (**Figure 2**).

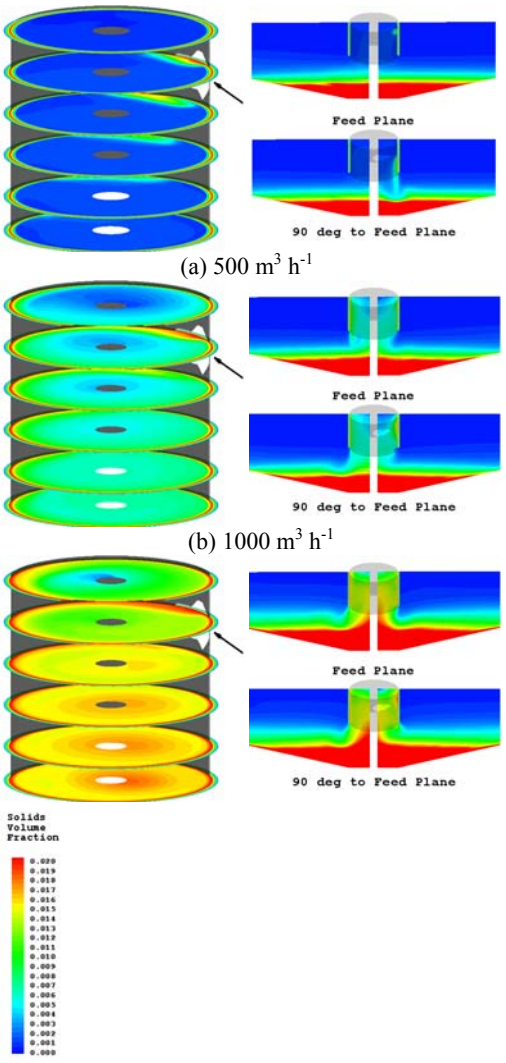

(a) 500 m^3 h^{-1}

(b) 1000 m^3 h^{-1}

(c) 2000 m^3 h^{-1}

Figure 3: PB-CFD model prediction of the solids distribution in the open feedwell (left) and in the entire thickener (right).

A region of high solids is shown at the base of the thickener in the bed region (**Figure 3**). Solids must build up in this region in order for the model to conserve mass, i.e. since all the feed solids reports to the underflow with only a portion of the liquid (remainder of the liquid goes to overflow), the solids must build up at the base. However, at this stage of the model development, the physics of sedimentation and compression are not fully included here.

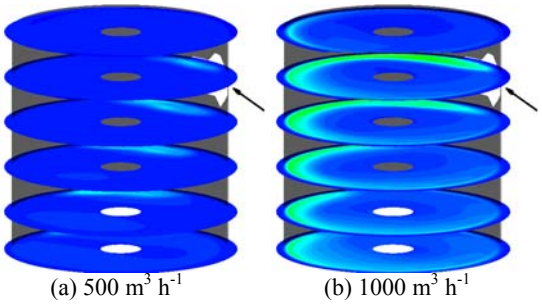

(a) 500 m^3 h^{-1} (b) 1000 m^3 h^{-1}

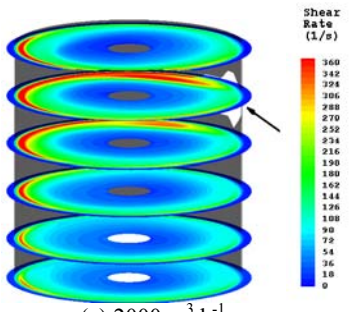

(c) 2000 m^3 h^{-1}

Figure 4: PB-CFD model prediction of shear rate in the feedwell.

One of the key variables affecting flocculation is the fluid shear rate, with a higher shear rate increasing the rates of flocculant mixing/adsorption, particle collision (aggregate growth) and also aggregate breakage. **Figure 4** shows the distribution of shear rate in the open feedwell model. It shows that the turbulence in the feedwell is not uniform and the shear rate varies from high inside the feed stream and near the inner walls to low elsewhere. As the flow rate is increased, the shear rate is higher and more uniformly distributed through the feedwell, increasing residence time, flocculant adsorption and aggregation.

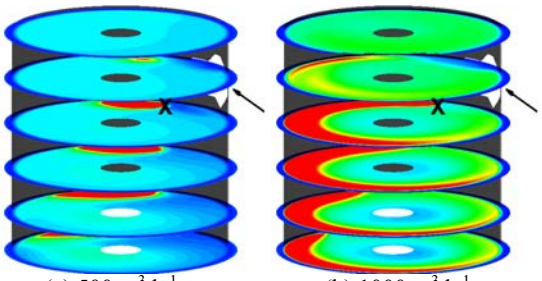

(a) 500 m^3 h^{-1} (b) 1000 m^3 h^{-1}

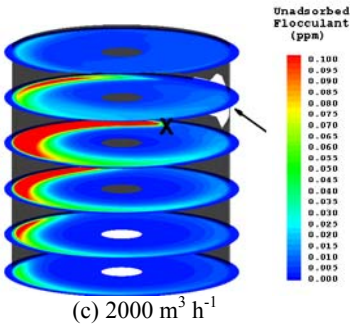

(c) 2000 m^3 h^{-1}

Figure 5: PB-CFD model prediction of the unadsorbed flocculant in the feedwell. The locations of the flocculant sparges are marked by an X.

In these simulations, the flocculant was added into the feed stream about 1 m downstream of the inlet as shown in **Figure 5**. For the case of low flow rate (500 m^3 h^{-1}), poor flocculant dispersion is again clearly evident, with high concentrations inside the feed stream from the flocculant entry point. Due to the low shear rate within the feedwell and short residence times, the flocculant is only partially adsorbed before exiting the feedwell. At the exit plane below the feedwell, there is a significant level of free flocculant left unadsorbed (almost 60% of the total input). A higher inlet velocity disperses the flocculant more uniformly throughout the feedwell. The reduction in unadsorbed flocculant is also significant with 14.7% and 0.2% unadsorbed for flow rates of 1000 and 2000 m^3 h^{-1}, respectively.

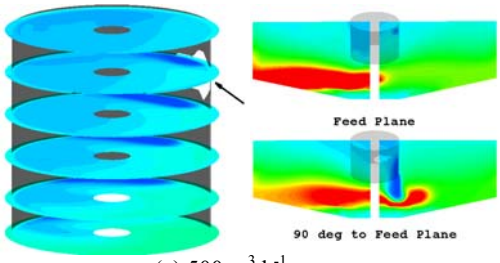

(a) 500 m^3 h^{-1}

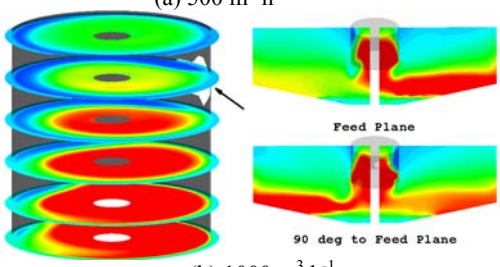

(b) 1000 m^3 h^{-1}

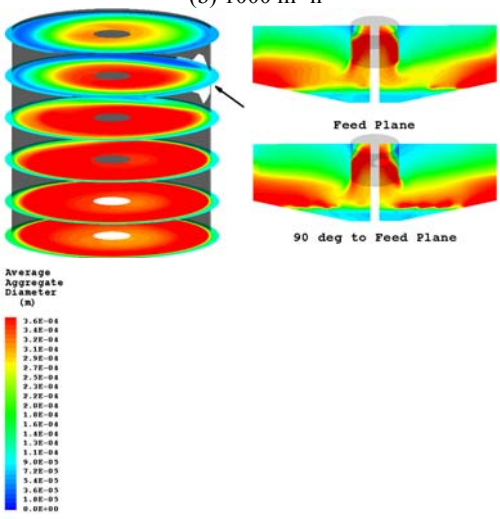

(c) 2000 m^3 h^{-1}

Figure 6: PB-CFD model prediction of the average aggregate size in the feedwell (left) and in the entire thickener (right).

Figure 6 shows the distribution of the average aggregate diameter predicted by the PB-CFD model for the feedwell, and the visualisation of particle aggregation is shown in **Figure 7**. At a flow rate of 500 m^3 h^{-1}, insufficient dispersion and mixing leads to limited aggregation inside the feedwell. Post-feedwell flocculation is dominant as the particle aggregation continues to occur outside the feedwell in the settling zone below the feedwell. The mean aggregate diameter produced at the low flow velocity is quite small, only 197 μm at the measurement plane (see **Figure 1**). When the flow rate is increased to 1000 m^3 h^{-1}, the feedwell performs better with improved solids/flocculant dispersion and mixing and therefore more aggregation with larger aggregates formed throughout the feedwell (mean size 270 μm at the measurement plane). The largest aggregates are produced in the centre of the feedwell, where solids and flocculant are recycled back inside by the dilution stream,

creating an enclosed flocculating region. This effect is seen again at the highest flow rate (2000 m^3 h^{-1}), where the sinking feed stream discharged from the feedwell forms an annular shield below it, recycling high solids and free flocculant back into the enclosed flocculating region which extends right up to the free surface. Under these conditions, the mean size calculated at the measurement plane is further increased to 294 µm.

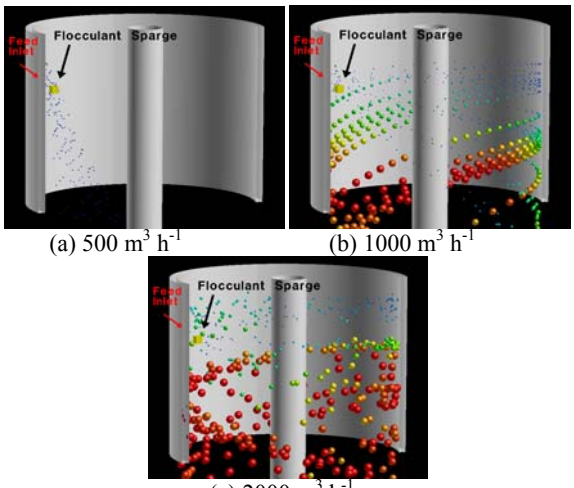

(a) 500 m^3 h^{-1} (b) 1000 m^3 h^{-1}

(c) 2000 m^3 h^{-1}

Figure 7: Visualisation of particle aggregation in the feedwell.

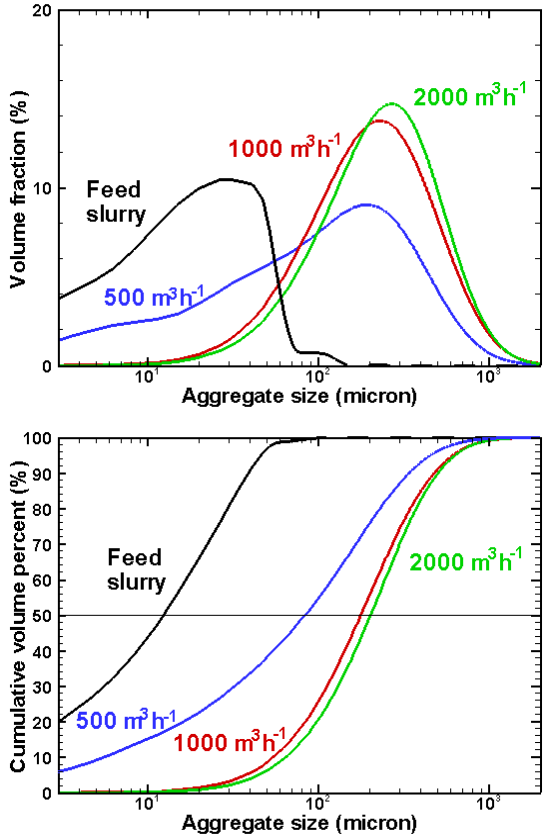

Figure 8: Size distributions for three flow rates in the feedwell predicted by the PB-CFD model at the measurement plane.

The size distributions predicted by the PB-CFD model for the feedwell are plotted in **Figure 8** (Note that the size distributions are calculated by integrating over the measurement plane in **Figure 1**). The primary feed particle size distribution is shown by the black curve. The aggregate size increases with the flow rate, the most significant improvement is obtained between 500 and 1000 m^3 h^{-1}. At the lowest flow rate, a large portion of the primary particles remain unflocculated after exiting the feedwell and the percentage of fines < 10 µm is quite high at 16%, compared to 0.22% and 0.20% for the higher flow rates. This is because at low flow rates the open feedwell has poor rates of flocculant mixing/adsorption, short residence time and less aggregate growth. Comparisons of the proportion of residual fines are a good indication of the likely relative overflow solids.

CONCLUSION

A population balance PB–CFD model has been used to describe fluid flow, solids distribution, and aggregation/breakage kinetics of flocculation in gravity thickeners. The simulation results using an open feedwell show remarkably varied behaviour with thickener throughput. At low flow rates, the feed plummeted through the feedwell with little mixing or flocculation, and the aggregates were still in the growth phase outside of the feedwell. At higher throughputs this particular open feedwell performed better, suggesting they were oversized for the lower throughputs. The sensitivity of the feedwell performance to throughput has implications for plants with fluctuating process streams and is also likely to have consequences for thickener control.

This study shows the nature of the results that can be obtained from the combined PB-CFD model under different conditions, and clearly demonstrates its power as a new tool for feedwell design and optimisation.

ACKNOWLEDGEMENT

This work was conducted as part of the AMIRA P266 'Improving Thickener Technology' series of projects. The authors wish to thank the following companies for their support:

Albian Sands Energy, Alcan International, Alcoa World Alumina, AngloGold Ashanti Australia, Anglo American, Bateman Process Equipment, BHP Billiton, Cable Sands, Ciba Specialty Chemicals, Cytec Australia Holdings, De Beers, GL&V Dorr Oliver, Glencore, Hatch, Iluka Resources, Kumba Resources, Lightnin Africa, Metso Minerals, Minara Resources, Mt Isa Mines, OMG Cawse, ONDEO Nalco, Outokumpu Technology Pty, Phelps Dodge Corporation, Queensland Alumina, Rio Tinto, Tiwest, Worsley Alumina and Zinifex Limited.

REFERENCES

Heath A.R. and Koh, P.T.L. 2003, 'Combined Population Balance and CFD Modelling of Particle Aggregation by Polymeric Flocculant', *Third International Conference on CFD in the Mineral and Process Industries.* CSIRO, Melbourne, Australia, pp. 339-344.

Heath, A.R., Bahri, P.A., Fawell, P.D. and Farrow, J.B. 2006A, 'Polymer Flocculation of Calcite: Population Balance Model', *AIChE Journal*, Vol. 52, No. 5, pp. 1641-1653.

Heath, A.R., Bahri, P.A., Fawell, P.D. and Farrow, J.B. 2006B, 'Polymer Flocculation of Calcite: Relating the Aggregate Size to the Settling Rate', *AIChE Journal*, Vol. 52, No. 6, pp. 1987-1994.

Richardson, J.F. and Zaki, W.N. 1955, 'Sedimentation and fluidisation', *Trans. Instn. Chem. Engrs*., Vol. 32, pp. 35-53.

Saffman, P. and Turner, J. 1956, 'On the collision of drops in turbulent clouds', *Journal of Fluid Mechanics*, Vol. 1, pp. 16-30.

Stokes, G.G. 1851, 'On the effect of the inertial friction of fluids on the motion of pendulums', *Trans. Cambridge Philos. Soc*., Vol. 9, pp. 8-106.

Šutalo, I.D., Nguyen, T., Rudman, M., 2000. Modelling studies of fluid flow in a thickener feedwell model. *CHEMECA 2000*, Perth, Western Australia, 9–12 July.

Šutalo, I.D., Nguyen, T., White, R.B., Rudman, M., 2001. Experimental and numerical investigations of the fluid flow in thickener feedwells, *Sixth World Congress of Chemical Engineering*, Melbourne, Australia, 23–27 September 2001, paper 941.

White, R.B., Šutalo, I.D., Nguyen, T., 2003, Fluid flow in thickener feedwell models. *Minerals Engineering* 16 (2), 145–150.